scientific reports

Check for updates

OPEN

Increased individual variability in functional connectivity of the default mode network and its genetic correlates in major depressive disorder

Chi Yao[1,2], Peng Wang[1], Yang Xiao[3], Yuhong Zheng[1], Jiayong Pu[1], Yongwei Miao[4], Jinghua Wang[1] & Shao-Wei Xue[1]✉

Major depressive disorder (MDD) is a highly heterogeneous psychiatric disorder characterized with considerable individual variability in clinical manifestations which may correspond to brain alterations including the default mode network (DMN). This study analyzed resting-state functional magnetic resonance imaging (rs-fMRI) data from 796 MDD patients and 823 healthy controls (HC) to investigate individual variability in functional connectivity (IVFC) between the DMN and 108 non-DMN regions. We aimed to identify MDD-related IVFC abnormalities and their clinical relevance, alongside exploring gene expression correlations. The results revealed similar spatial patterns of IVFC within the DMN in both groups, yet significantly increased IVFC values in MDD patients were observed in regions such as the ventromedial prefrontal cortex, anterior cingulate cortex, posterior cingulate cortex, fusiform gyrus, and occipital cortex. Notably, the mean IVFC in the DMN and fusiform gyrus was positively correlated with Hamilton Rating Scale for Depression (HAMD) scores in MDD patients. Gene expression analyses explained 47.0% of the variance in MDD-related IVFC alterations, with the most associated genes enriched in processes including membrane potential regulation, head development, synaptic transmission, and dopaminergic synapse. These findings highlight the clinical importance of IVFC variability in the DMN and suggest its potential role as a biomarker in MDD.

Keywords Individual variability, Heterogeneity, Default mode network, Major depressive disorder, Resting-state fMRI

Major depressive disorder (MDD) is a prevalent psychiatric condition with considerable heterogeneity, encompassing symptoms ranging from diminished interest and pleasure to recurrent suicidal ideation, often accompanied by physical and cognitive dysfunction[1,2]. This diversity presents challenges in establishing standardized diagnostic criteria and developing effective treatments[3]. The variability in MDD is reflected in distinct symptom profiles, clinical trajectories, and treatment responses across individuals, complicating the identification of reliable biomarkers for diagnosis and prognosis. Recent advances in neuroscience have highlighted the pivotal role of alterations in brain structure and function, particularly within neural circuits implicated in emotion regulation and cognitive control, in elucidating the pathophysiology of MDD[2]. However, the mechanisms linking these neural changes to the clinical heterogeneity in MDD remain unclear. Elucidating these pathways is essential to improving our comprehension of MDD and fostering the development of more targeted, personalized, and efficacious diagnostic and therapeutic approaches.

One brain network that has attracted significant interest in this context is the default mode network (DMN). The DMN, which comprises various brain regions, exhibits a distinctive pattern of activity modulation, characterized by a reduction in activity during tasks requiring sustained attention and an increase in activity during introspective mental processes[4–6]. Dysfunction in the DMN had been linked to a number of mental

[1]Center for Cognition and Brain Disorders/Department of Neurology, The Affiliated Hospital, Hangzhou Normal University, No.2318, Yuhangtang Rd, Hangzhou, Zhejiang, China. [2]Jing Hengyi School of Education, Hangzhou Normal University, Hangzhou, China. [3]Peking University Sixth Hospital, Peking University, Beijing, China. [4]School of Information Science and Technology, Hangzhou Normal University, Hangzhou, China. ✉email: xuedrm@126.com

health issues, including MDD[7]. It was hypothesized that this dysfunction contributed to maladaptive rumination by preventing disengagement from intrusive, non-task-related thoughts[8]. While the DMN's influence on MDD had been consistently demonstrated[9–11], studies examining DMN dysregulation in MDD produced conflicting results[12], likely reflecting high heterogeneity within the DMN.

Recent advancements in neuroimaging techniques, particularly those utilizing functional magnetic resonance imaging (fMRI), have significantly enhanced our ability to measure intersubject variability and map the brain mechanisms underlying the clinical heterogeneity of MDD. Previous studies developed the individual variability of functional connectivity (IVFC) method for the purpose of characterizing the biological heterogeneity[13]. Researches indicated that the distribution of IVFC across the brain was non-uniform, with higher variability observed in multimodal cortical areas compared to primary cortical regions, a pattern consistent across both neonates and healthy adults[13–15]. Furthermore, higher IVFC has been positively correlated with higher-order brain functions, suggesting that increased variability may reflect enhanced cognitive capacities[16].

In MDD, altered whole-brain IVFC patterns have been observed, particularly involving inter-network connectivity in DMN[17]. These findings emphasized the potential role of altered functional connectivity variability in the neuropathology of MDD and underscored the importance of investigating IVFC as a biomarker for cognitive and behavioral variability in this disorder. However, the heterogeneity of IVFC of the DMN remains underexplored, especially in the context of mental health disorders. Further research is needed to clarify the neurophysiological mechanisms underlying MDD's clinical variability and diverse manifestations.

A previous study identified an association between IVFC and the gene expression of human accelerated regions[16], while another demonstrated that IVFC mediates the relationship between gene expression and depression severity[17]. The microarray dataset of the Allen Human Brain Atlas (AHBA) offers a valuable resource for investigating the correlation between microscopic-scale transcriptomic genes and macroscopic brain changes[18]. Investigating these genetic factors-brain alterations associations may facilitate clarify the specific brain alterations observed in MDD from a molecular perspective. Considering these findings, we aimed to examine the potential link between MDD-related DMN IVFC alterations and gene expression.

The present study aimed to elucidate the IVFC patterns of the DMN and its clinical implications, as well as its genetic association in MDD patients. Given the extensive involvement of the DMN in MDD and its multimodal properties, we hypothesized that MDD patients would exhibit significantly increased IVFC in DMN compared to healthy controls. This research sought to advance understanding of the biological heterogeneity underlying MDD, paving the way for individualized clinical diagnosis and tailored treatment strategies.

Methods and materials

Participants

The demographic and clinical profiles of the study participants are concisely presented in Table 1. The sample data utilized in this study were sourced from a rigorously quality-controlled, publicly accessible dataset contributed by the REST-meta-MDD project[19], which is part of the DIRECT Consortium[20] and available at (http://rfmri.org/REST-meta-MDD). MDD diagnoses were confirmed in accordance with the criteria outlined in either the Diagnostic and Statistical Manual of Mental Disorders, Fourth Edition (DSM-IV) or the International Classification of Diseases, 10th Revision (ICD-10). The severity of depressive symptoms was quantified using the 17-item Hamilton Depression Rating Scale[21]. The healthy controls (HC) consisted of individuals with no history of Axis I psychiatric or neurological disorders, either current or past.

As shown in Fig. 1, the participants from the REST-meta-MDD project were rigorously screened using stringent inclusion and exclusion criteria, aligning with previous studies[19,22]. Specifically, Site 4 and Site 25 were excluded from the current analysis due to participant duplication between Site 4 and Site 14, as well as an excessively high proportion of late-onset depression cases (mostly > 60 years old) and remitted patients at Site 25. Participants were subsequently disqualified if they: (1) lacked data on sex, age, or education; (2) were under 18 or over 65 years old; or (3) exhibited excessive head motion, defined as a mean framewise displacement (FD) exceeding 0.2 mm. Additionally, MDD patients were excluded if their 17-item Hamilton Rating Scale for Depression (HAMD) scores were below 8 points. Participants were also excluded if they had visually identified imaging distortions or missing signals in any region of interest (ROI) from the Dosenbach atlas[23] used in this

Characteristics	MDD (mean ± SD)	HC (mean ± SD)	t/χ^2	*p*
Sex (M/F)	796 (289/507)	823 (332/491)	2.785	0.095[a]
Age (years)	35.127 ± 11.914	35.033 ± 13.332	0.150	0.881[b]
Mean FD	0.068 ± 0.037	0.071 ± 0.038	−1.556	0.120[b]
Education level (years)	11.755 ± 3.430	13.315 ± 3.446	−9.127	< 0.001[b]
HAMD scores	22.275 ± 5.619			
HAMA scores[c]	20.415 ± 8.631			
Durations of illness (months)[d]	38.522 ± 62.938			

Table 1. Demographic data and group differences. *MDD* major depressive disorder, *HC* healthy controls, *SD* standard deviation, *M* male, *F* female, *HAMD* 17-item Hamilton Rating Scale for depression, *HAMA* 17-item Hamilton Rating Scale for anxiety, *FD* framewise-displacement. [a]The *p*-value was obtained by a chi-square test. [b]The *p*-value was obtained by a two-tailed two-sample *t*-test. [c]Data on the HAMA scores was available for 544 patients. [d]Data on the duration of illness was available for 691 patients.

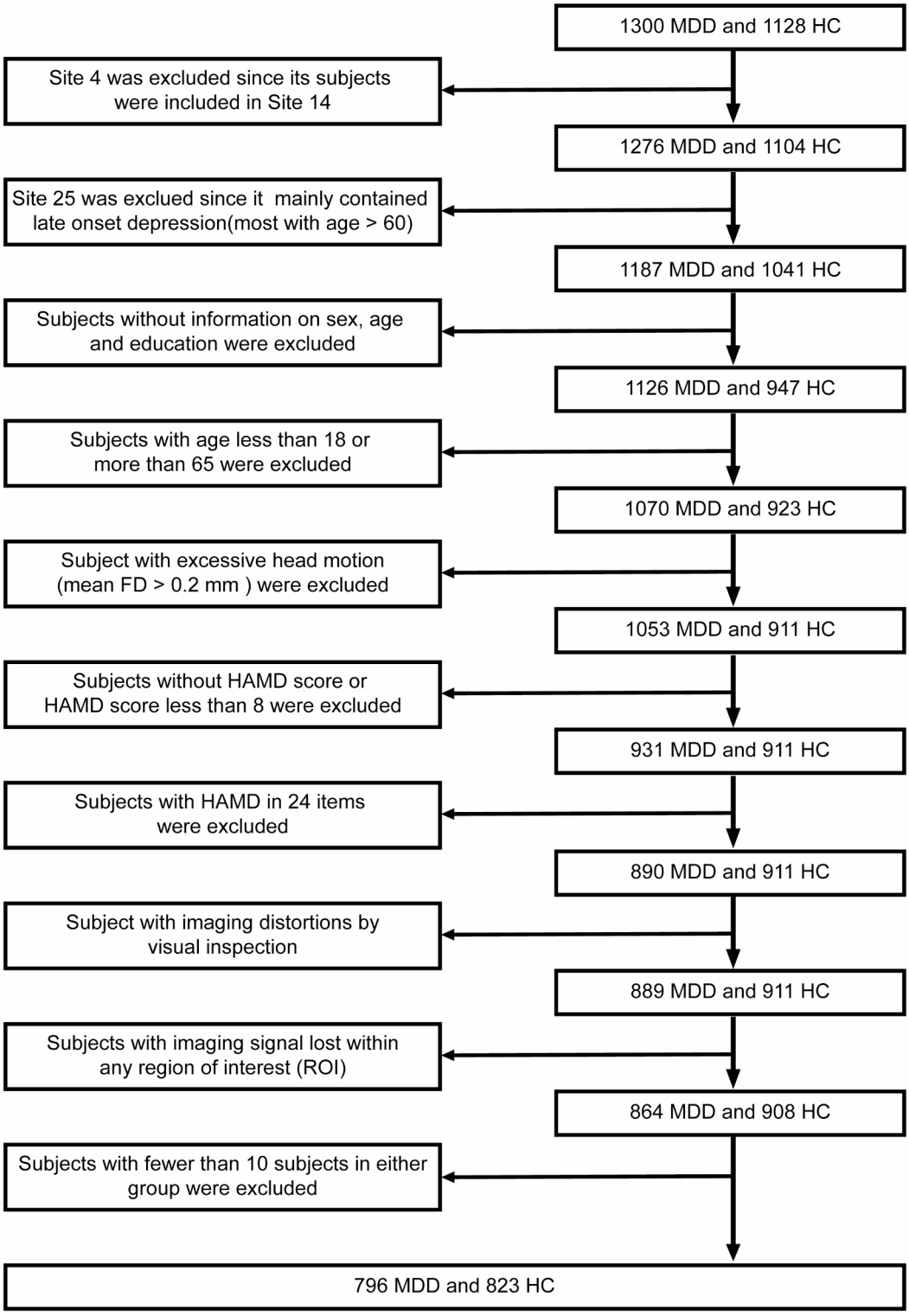

Fig. 1. The flowchart outlining the exclusion process of subjects and the labels assigned to excluded subjects at each stage of the process. *MDD* major depressive disorder, *HC* healthy controls.

study. To balance sample size optimization with minimizing extreme biases, sites with fewer than 10 MDD patients or 10 HC subjects were not considered in the analysis.

Ethical considerations

The study was conducted in full compliance with the ethical principles set forth in the Helsinki Declaration and received approval from the Institutional Review Boards (IRB) at all participating sites. All subjects provided written informed IRB-approved consent before participating in the formal testing at their local institution.

Data preprocessing

Brain image processing was performed in accordance with a standardized protocol[19] utilizing the DPARSF software (accessible at http://www.rfmri.org/). To ensure signal stabilization and allow for environmental adaptation, the initial ten functional volumes were excluded. The remaining images were corrected for temporal shifts between different acquisitions within each volume and realigned to the first volume to minimize head motion artifacts. The corrected images were then normalized to the standard Montreal Neurological Institute (MNI) space with a voxel size of 3 mm × 3 mm × 3 mm. Nuisance regression was applied to remove Friston-24 motion parameters, as well as signals from white matter and cerebrospinal fluid (CSF). Finally, temporal bandpass filtering was conducted, restricting the frequency range to 0.01–0.10 Hz to capture biologically relevant fluctuations.

Gene expression data and preprocessing

Gene expression data for this study were obtained from six neurotypical adult donors provided by the Allen Human Brain Atlas[24] (AHBA; http://human.brain-map.org). The preprocessing of gene microarray data from brain tissue samples followed the recommended pipeline[25] of the abagen toolbox (https://www.github.com/netneurolab/abagen). The microarray data was mapped onto a parcellation with 34 DMN brain regions defined by Dosenbach atlas[23]. After pre-processing, a gene expression matrix (34 DMN regions × 15,632 genes) was generated for subsequent transcription-neuroimaging association analysis.

Characterizing individual variability in the default mode network

Following previous procedure proposed by Mueller et al.[13], the IVFC value of ROI i was defined as follow:

$$\mathrm{IVFC}_i = 1 - \frac{\sum \left[corr\left(F_i\left(s_p\right), F_i\left(s_q\right)\right)\right]}{m\left(m-1\right)}, p, q = 1?m; p \neq q.$$

where p and q are both subjects in the MDD or HC groups; m is the number of subjects in the dataset; s indicates the subject; and $F_i\left(s_p\right)$ is the functional connectivity profile of region i of subject p; the $corr$ is Pearson's correlation between the functional connectivity of two subjects.

The existence of individual differences (including cognitive and behavioral differences) among humans is partially attributed to differences in brain function and structure (see Fig. 2A). In this study, the individual variability of functional connectivity (IVFC) in the the default mode network (DMN) was computed based on the functional connectivity between the 34 DMN regional seeds (Fig. 2B) towards 108 non-DMN cerebral regions generated using the Dosenbach atlas[23] (Fig. 2C). Specifically, the DMN-cerebral functional connectivity for each participant was first measured using Pearson's correlation analysis between the time series of each DMN seed and the time series of non-DMN cerebral regions. The correlation coefficient was then normalized using Fisher's z-transformation to improve its normality, followed by a z-score transformation (subtracting the mean and dividing by the standard deviation) to ensure comparability across measures. We applied the Combat technique to adjust for site effects in the functional connectivity matrices, with sex, age, education, and mean framewise displacement considered as biological covariates of interest and the empirical Bayes procedure employed a default non-parametric prior method[26]. For one of the 34 DMN ROIs, each subject had a 108-unit functional connectivity vector with another 108 non-DMN cerebral ROIs. By correlating these vectors across all subjects within each group, we generated a subject-to-subject similarity matrix. The IVFC for a DMN ROI was then estimated by subtracting the average similarity (calculated per subject as the mean similarity with all other subjects) from one. For the 34 DMN ROIs, this process yields a matrix with dimensions corresponding to the number of ROIs and the number of subjects. Each DMN ROI has a functional connectivity (FC) vector with other ROIs, and the IVFC value represents the average dissimilarity between an individual's FC distribution and those of other subjects. These IVFC values derived from functional connectivity can explain significant variations in cognitive and behavioral functions among individuals within the same group.

Statistical analysis

We performed nonparametric permutation tests to compare DMN IVFC profiles between MDD and HC groups. All participants were combined into a single pool, and group labels were randomly shuffled before splitting the participants into two new groups. IVFC patterns and their differences were then recalculated for each permutation. This procedure was repeated 10,000 times to create a null distribution. The p-value was calculated as the proportion of the null distribution that exceeded the observed group difference. To examine the relationship between IVFC and clinical variables in MDD, we performed partial correlation analyses, controlling for age, sex, educational level, and mean framewise displacement (FD) as covariates. The IVFC measures included both the overall mean IVFC across the entire DMN and the IVFC values of five significantly altered DMN regions. Clinical variables analyzed in this study comprised HAMD-17 scores, HAMA scores, and illness duration. Statistical significance was determined using a Bonferroni correction for multiple comparisons, with a threshold set at $p < 0.05$.

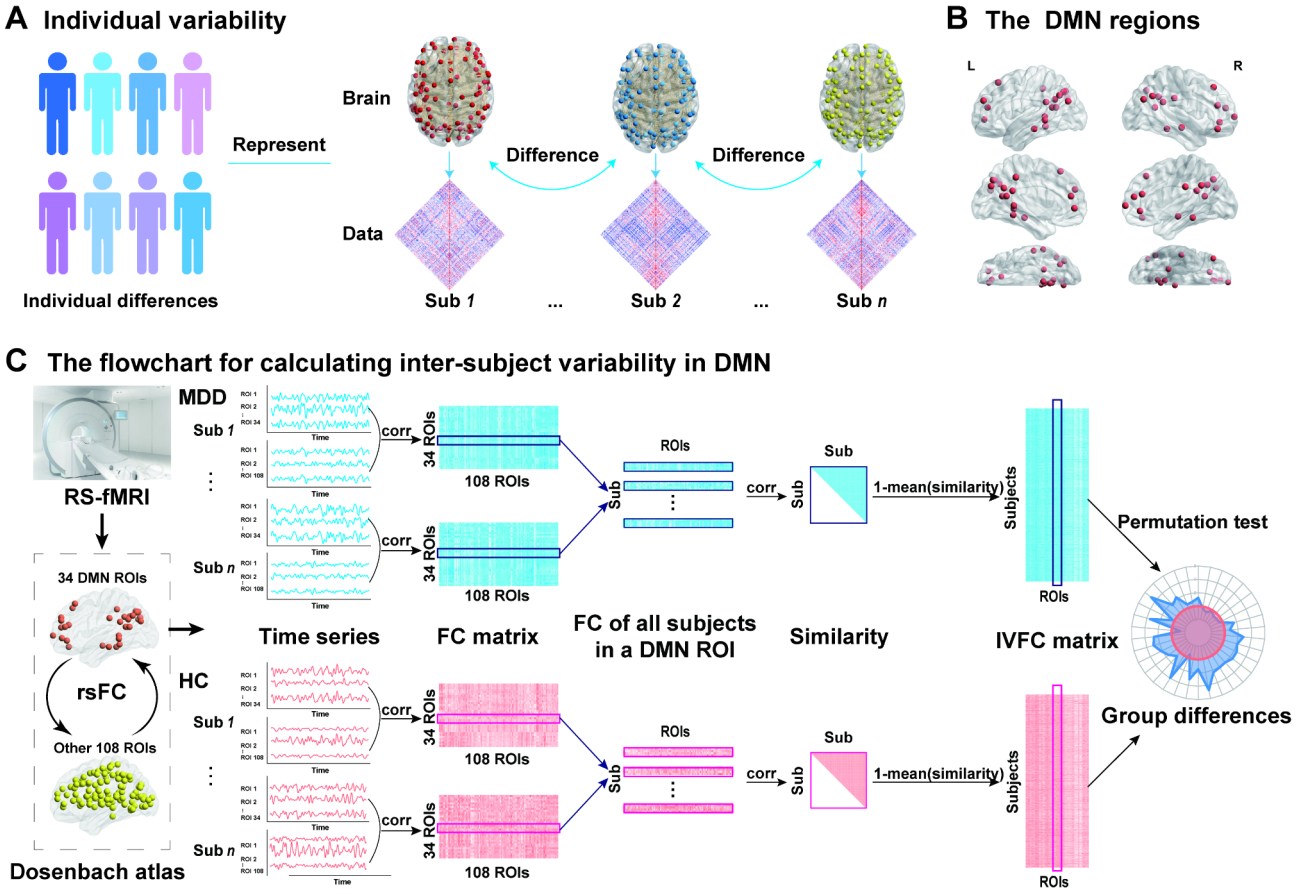

Fig. 2. Conceptual overview of the individual variability of functional connectivity (IVFC) between the DMN and other cerebral regions. (**A**) The individual variability. There are extensive behavioral differences among individuals, and behavioral differences are partially represented by differences in the brain. (**B**) The 34 DMN regions segmented utilizing the Dosenbach atlas. (**C**) The flowchart depicting the methodology for calculating individual variability based on the functional connectivity between the DMN and other cerebral regions. *DMN* default mode network, *Sub* subject, *RSFC* resting-state functional connectivity, *MDD* major depressive disorder, *HC* healthy controls, *Corr* correlation, *ROI* region of interest, *FC* functional connectivity, *IVFC* individual variability of functional connectivity.

Transcription-neuroimaging association analysis

To investigate the genetic associations with MDD-related IVFC changes, we applied partial least squares (PLS) regression. The z-score normalized gene expression matrix (34 DMN regions × 15,632 genes) served as the predictor variable, while the z-score normalized Z-values from the between-group IVFC comparisons were used as the response variable. Statistical significance was determined using a spatial autocorrelation-corrected permutation test (10,000 iterations) with spherical rotations[27]. For each significant component, a spatial correlation between the weighted gene expressions and the Z-value map was performed and corrected with a spatial autocorrelation-corrected permutation analysis (10,000 times). The PLS weight for each gene was transformed into *z*-scores by dividing each weight by the standard deviation obtained from 10,000 bootstrap times. Genes were ranked by their z-scores, and univariate one-sample Z tests were employed to assess statistical significance. Genes passing the 1% false discovery rate (FDR) threshold were classified as PLS+ (positive weights) or PLS– (negative weights). In order to elucidate the biological significance of the PLS gene list, gene enrichment analyses were conducted using Metascape (https://metascape.org/gp/index.html#/main/step1), utilising the Gene Ontology (GO) Bioprocesses and Kyoto Encyclopedia of Genes and Genomes (KEGG) pathway databases. The enriched pathways were corrected to a 5% false discovery rate (FDR) correction to ascertain their statistical significance.

Results

Individual variability in the default mode network

As illustrated in Fig. 3A, the results revealed a remarkable similarity in the spatial distribution pattern of IVFC within DMN regions between MDD patients and HC ($r = 0.9841$, $p < 0.001$). Notably, the peak IVFC values were observed in the ventromedial prefrontal cortex (vmPFC), while the lowest values were found in the intraparietal sulcus (IPS). However, MDD patients demonstrated a rightward shift in the IVFC density distribution

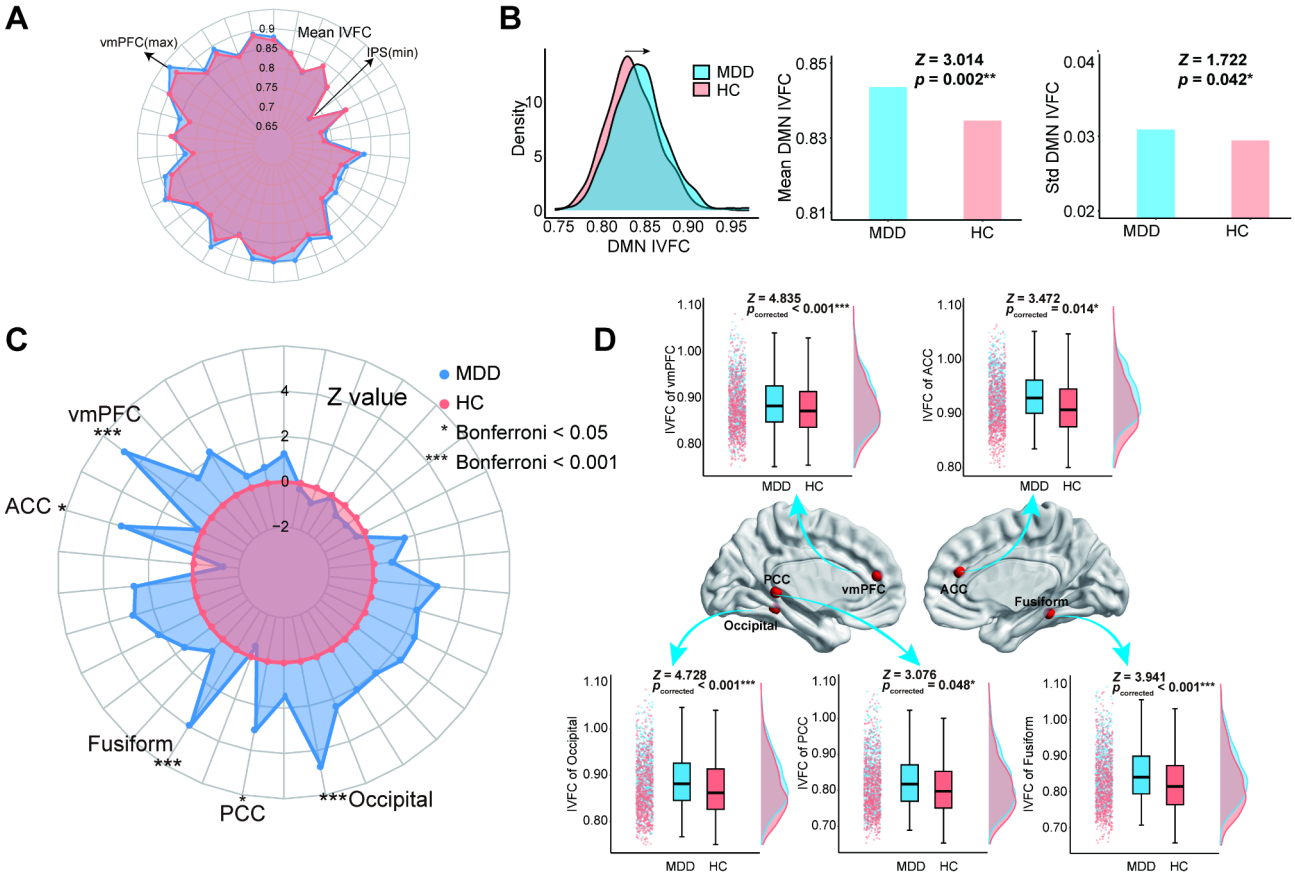

Fig. 3. The alterations of individual variability in MDD patients. (**A**) The mean IVFC spatial patterns of the DMN regions. (**B**) The different DMN IVFC patterns of the MDD and HC groups, including density, mean, and standard deviation values. (**C**) The *Z*-value patterns of the DMN regions. The z-value for each ROI was obtained through between-group comparisons using the permutation test. (**D**) The subregions of the DMN exhibited altered IVFC patterns. A comparison was conducted between the density distribution and the mean IVFC values across the DMN regions. ***$p < 0.001$; **$p < 0.01$; *$p < 0.05$; *IVFC* individual variability of functional connectivity, *Std* standard deviation, *MDD* major depressive disorder, *HC* healthy controls, *vmPFC* ventromedial prefrontal cortex, *IPS* intraparietal sulcus, *ACC* anterior cingulate cortex, *PCC* posterior cingulate cortex, *DMN* default mode network.

MNI	Brain region	DIVFC	$p_{corrected}$	Cohen's d
− 11, 45, 17	vmPFC	0.022	< 0.001	0.484
9, 39, 20	ACC	0.027	0.014	0.341
28, − 37, − 15	Fusiform gyrus	0.022	< 0.001	0.393
− 8, − 41, 3	PCC	0.018	0.048	0.304
− 28, − 42, − 11	Occipital	0.028	< 0.001	0.475

Table 2. Brain regions with significant differences in IVFC between MDD and HC. *DIVFC* differences in IVFC, $p_{corrected}p$ Bonferroni corrected, *vmPFC* ventromedial prefrontal cortex, *ACC* anterior cingulate cortex, *PCC* posterior cingulate cortex.

compared to healthy controls (Fig. 3B), indicating significantly increased IVFC values, both in terms of the mean ($Z = 3.014$, $p = 0.002$) and standard deviation ($Z = 1.772$, $p = 0.042$). As depicted in Fig. 3C,D, MDD patients exhibited significantly elevated regional IVFC values compared to HC in several crucial regions, including the vmPFC ($Z = 4.835$, $p < 0.001$, Bonferroni corrected, Cohen's d = 0.484), ACC ($Z = 3.472$, $p = 0.014$, Bonferroni corrected, Cohen's d = 0.341), fusiform gyrus ($Z = 3.941$, $p < 0.001$, Bonferroni corrected, Cohen's d = 0.393), PCC ($Z = 3.076$, $p = 0.048$, Bonferroni corrected, Cohen's d = 0.304), and occipital cortex ($Z = 4.728$, $p < 0.001$, Bonferroni corrected, Cohen's d = 0.475). A summary of these findings can be found in Table 2.

Relationship between IVFC and clinical variables in MDD

As shown in Fig. 4, there was a statistically significant association between the mean IVFC values of the DMN in MDD patients and HAMD scores ($r = 0.071$, $p = 0.043$). At the regional level within the DMN, a positive correlation was observed between the IVFC values in the fusiform gyrus and HAMD scores ($r = 0.096$, $p = 0.033$, Bonferroni corrected). Besides, there were correlations between the IVFC values of the ACC and illness duration ($r = -0.094$, $p = 0.0136$, uncorrected), between the IVFC of the PCC and HAMA scores ($r = -0.1016$, $p = 0.0182$, uncorrected).

Results of transcription-neuroimaging association analysis

Figure 5 presents the results of the transcription-neuroimaging association analysis. Figure 5A illustrates the distribution of Z-values on the left and the distribution of PLS1 gene scores on the right. For subsequent analysis, we concentrated on PLS1, which accounted for 47.0% of the variance in gene expression. ($p_{spin} = 0.038$). The spatial distribution of gene expression exhibited a pattern characterised by lower expression levels in the anterior DMN regions and higher expression levels in the posterior DMN regions. A significant positive correlation was observed between PLS1 scores and Z-value patterns ($r = 0.68$, $p_{spin} < 0.001$, Fig. 5A, middle). After performing univariate one-sample Z-tests, 941 genes with positive weights (PLS1+) and 531 genes with negative weights (PLS1-) were identified, both at a false discovery rate (FDR) threshold of 1%, with only PLS1 + showing significant gene enrichment results. The PLS1 + genes were found to be enriched in several key biological processes, including "regulation of membrane potential," "head development" and "modulation of chemical synaptic transmission". Moreover, KEGG pathway enrichment analysis revealed associations with the "Dopaminergic synapse" and "Retrograde endocannabinoid signaling" pathways (Fig. 5B).

Discussion

In this study, we quantitatively assessed the heterogeneity of the default mode network (DMN) by analysing individual variability in functional connectivity (IVFC) between the DMN regions and non-DMN cerebral regions. Subsequently, we sought to elucidate the clinical implications of this heterogeneity in MDD patients. The principal findings of this study were as follows: First, although MDD patients and HC exhibited a similar spatial distribution of DMN IVFC, MDD patients exhibited significantly higher mean and standard deviation values of IVFC. Second, MDD patients demonstrated markedly increased IVFC in five DMN regions compared to HC, specifically in the vmPFC, ACC, PCC, fusiform gyrus, and occipital cortex. Third, the mean IVFC values of the DMN and the fusiform gyrus were significantly positively correlated with HAMD scores in MDD patients. These findings provided evidence of heightened variability in the functional integration related to the DMN among patients with MDD and underscored the importance of exploring DMN variability in MDD research.

A consistent spatial distribution pattern of IVFC was observed across 34 DMN regions in both MDD patients and HC. Specifically, the vmPFC and intraparietal sulcus (IPS) exhibited the highest and lowest IVFC values, respectively. Importantly, as a pivotal brain region implicated in MDD, the vmPFC displayed a notably high degree of heterogeneity across the patient population, suggesting potential variations in its functional integration that may underlie MDD. This finding aligned with previous studies[17,28], suggesting that the fundamental

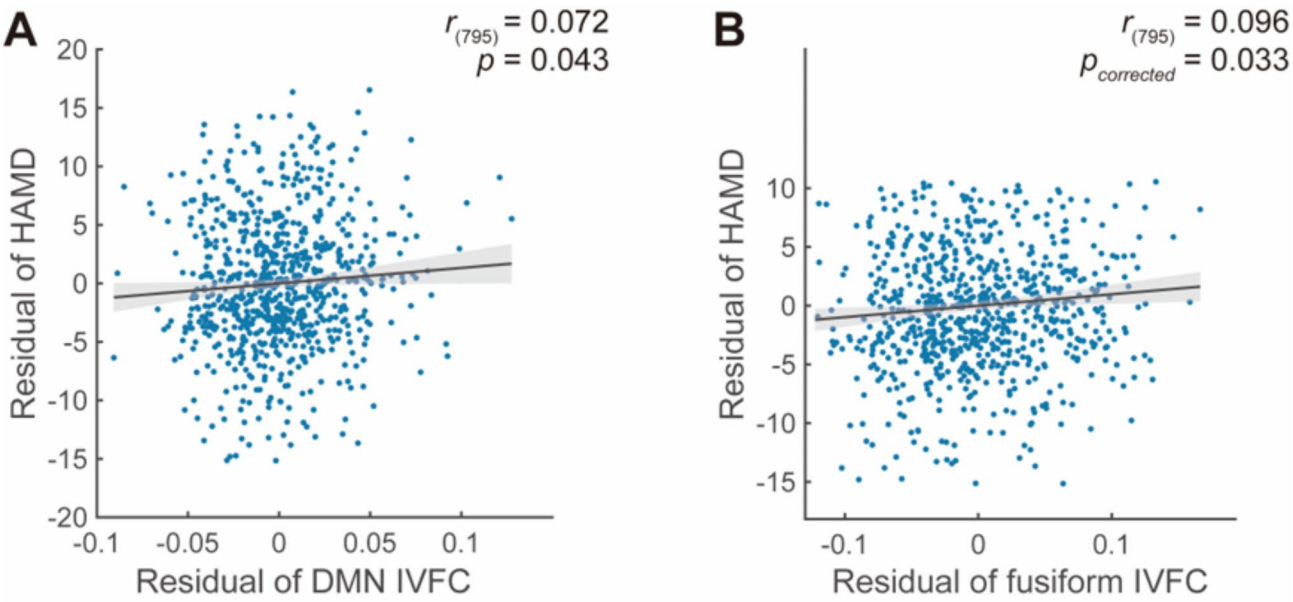

Fig. 4. The partial correlation analysis of IVFC and HAMD scores (**A**) The correlation between HAMD scores and the mean IVFC of DMN in MDD patients. (**B**) The correlation between HAMD scores and IVFC of the fusiform gyrus in MDD patients. *HAMD* Hamilton Rating Scale for depression, *IVFC* individual variability of functional connectivity, *DMN* default mode network.

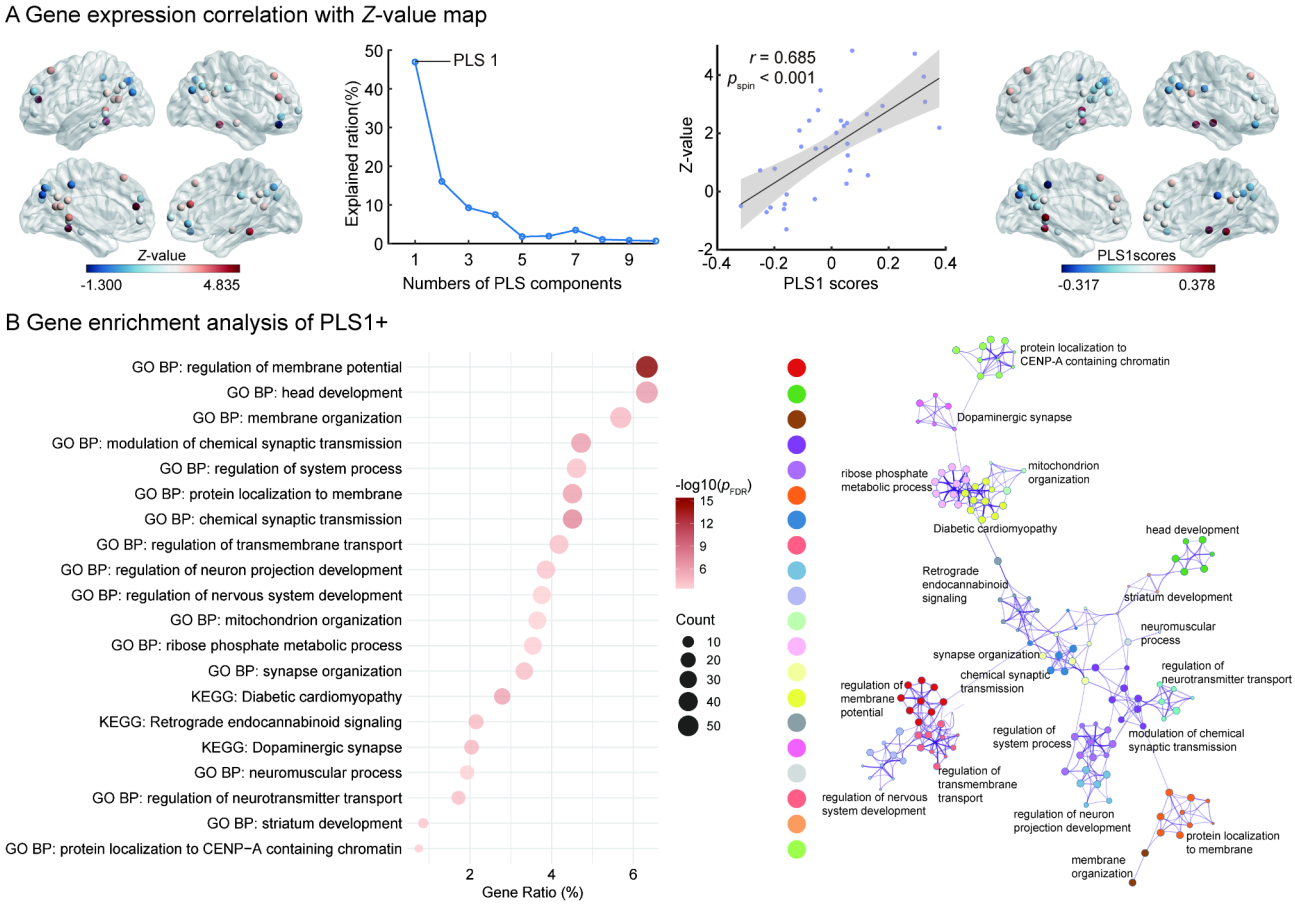

Fig. 5. Gene expression profiles related to MDD-related IVFC alterations. (**A**) Regional mapping of PLS1 scores and Z-values (both sides). The z-values were obtained from between-group comparisons of IVFC for MDD and HC. Explained variance of each PLS component and the correlation between PLS1 scores and Z-map (middle). (**B**) Left: Bubble plot of top 20 enrichment analysis results. This bubble plot illustrates the functional annotations for PLS1 + genes based on Gene Ontology (GO) terms and Kyoto Encyclopedia of Genes and Genomes (KEGG) pathways. The size of each bubble reflects the number of genes that are shared between the given term and the other terms shown, while the color bar represents the Benjamini–Hochberg False Discovery Rate (BH-FDR) corrected *p*-value. Right: Network of enriched terms. This network derived from Metascape, features nodes representing individual pathways, color-coded by cluster to indicate potential functional relationships, on the left side of this network enriched terms, dots were used to represent the color of each cluster, and these are matched with the terms in the left bubble plot.

organization of the DMN remained intact in MDD. The elevated mean IVFC values in MDD patients indicated greater heterogeneity in DMN functional connectivity, which may reflect increased randomized functional connectivity[29], which might have led to a more discrete distribution of functional connectivity. Contrary to previous research that suggested reduced variability as a marker of dedifferentiation in psychiatric conditions[30], our results revealed an increased standard deviation in IVFC within the DMN of MDD patients, suggesting to a more complex and region-specific disruption. This discrepancy may have been attributed to our focused methodological approach, emphasizing inter-network analyses between DMN and non-DMN regions. By minimizing potential confounding factors related to intra-network homogeneity, our approach provided a more nuanced, DMN-centric depiction of functional variability, revealing distinct and potentially pathognomonic patterns specific to MDD.

This elevated IVFC was particularly pronounced in five DMN regions: the vmPFC, ACC, PCC, fusiform gyrus, and occipital cortex. IVFC values represent the average difference between an individual's FC distribution and that of others, where the FC distribution is simply the FC between a DMN ROI and all other brain ROIs in present study. If the IVFC of the MDD increases, it means that the FC distribution of the MDD is more inconsistent. The vmPFC, a crucial region implicated in emotional regulation, reward processing, and decision-making[31], was characterised by substantial inter-individual variability, may underlined differential responses to emotional stimuli[32,33] and decision-making tasks among individuals[34]. This variability was particularly relevant in MDD, where vmPFC dysfunction may have contributed to anhedonia[35–37], a core symptom of depression, complicating treatment outcomes and underscoring the need for personalized therapeutic approaches. The elevated IVFC of the vmPFC observed in our study was consistent with previous whole-brain IVFC

analyses[17], thereby underscoring the vmPFC's potential role in MDD pathophysiology. The ACC, crucial for emotion regulation, pain processing and decision-making[38,39], had been extensively linked to depression and antidepressant treatment response[40,41]. Abnormalities in the functional connectivity and decreased flexibility of ACC had been reported in MDD patients[42,43]. The ACC, a key region involved in emotion regulation, pain processing, and decision-making, has been extensively associated with depression and treatment response. Prior research has reported reduced functional flexibility and abnormal connectivity of the ACC in MDD patients. The observed increase in functional heterogeneity across MDD patients may indicate distinct sub-patterns of altered connectivity, which could be linked to variability in symptom domains such as emotional regulation, negative affect, and decision-making. The fusiform gyrus, involved in facial and body recognition, and within-category identification[44]. Specifically, the right fusiform gyrus, which was crucial for automatic face processing[45], had been implicated in the negative bias towards facial expressions observed in depression[46]. In MDD, decreased cortical folding[47] in right fusiform gyrus had been reported, which may have affected its ability to process visual information and impaired cognitive control. The fusiform gyrus also exhibited increased functional heterogeneity in MDD, which may have impaired its ability to accurately recognize facial expressions and emotional intensity, potentially leading to exaggerated negative emotions and social impairment in MDD patients. The PCC, central to the DMN, played a pivotal role in self-referential processing and attention regulation[48]. Altered functional connectivity in the PCC had been reported in a wide range of neurological and psychiatric disorders, including MDD, where it had been correlated with symptom severity[49] and illness duration[50]. The increased IVFC observed in the PCC may indicate disruptions in cognitive control and deficits in emotional regulation in MDD patients[51]. The occipital cortex, another region where alterations in IVFC were observed, had been highlighted in various studies showing decreased activity in MDD[52–54]. The increased IVFC in the occipital cortex may further emphasized the widespread impact of MDD on brain function and highlighted the potential role of the occipital cortex as a candidate biomarker for the disorder[55].

Importantly, our partial correlation analysis revealed a positive association between IVFC patterns in the DMN and the right fusiform gyrus with HAMD scores, aligning with previous studies[17,56] showing that increased IVFC in MDD patients reflects the severity of depressive symptoms. This relationship provides a potential explanation for the increased IVFC observed in MDD patients. Specifically, as the severity of depressive symptoms intensifies, patients may exhibit greater variability in functional connectivity patterns, reflecting a disruption in the brain's intrinsic functional organization may contributing to cognitive and emotional deficits. The right fusiform gyrus, which is involved in face processing and social cognition, showed significant variability linked to depression severity. This altered functionality may impair social interactions, further exacerbating depressive symptoms. These findings underscore the potential of IVFC as a biomarker for depression severity and highlight the need to account for clinical variability when investigating functional brain alterations in MDD.

A substantial body of research, including family, twin and adoption studies, had elucidated the complex genetic underpinnings of major depressive disorder[57]. Using transcriptional-neuroimaging spatial correlation analysis, we identified significant spatial correlations between IVFC changes and specific gene expression patterns. Genes with positive PLS1 weights were significantly enriched in a number of different GO biological processes and KEGG pathways. The GO biological processes we identified were predominantly related to the structure and function of membranes and synapses. This is consistent with previous findings on membrane abnormalities in depressed patients, such as abnormal membrane potential regulation that may be associated with chronically elevated levels of polyamines, which are associated with depression and suicide[58]; and localisation of proteins on membranes that may affect protein function and synaptic channels, which determine protein function and synaptic throughput in neurons[59]. Previous studies have also highlighted the key role of synaptic integrity in the pathogenesis of MDD[60], and many of the molecular pathways of depression may be synapse-related[61]. Furthermore, the KEGG pathway at dopaminergic synapses is similar to GO biological processes, which is consistent with previous studies and supports the importance of synapses in depression. The IVFC changes observed in depressed patients may result from alterations in neuronal membranes and synapses. Our findings highlight the critical role of gene expression in the regulation of these depression-related IVFC changes, thereby deepening our understanding of the underlying mechanisms. While our analysis provides insights into the potential genetic basis of MDD-related IVFC alterations, we caution that the identified gene expression patterns suggest vulnerability rather than direct causal links. Further within-subject studies assessing the relationship between genetic and IVFC alterations will be needed.

While these findings provided new insights into the role of DMN variability in MDD, several limitations must be acknowledged. Our study was dependent on the Dosenbach atlas for the selection of DMN regions, and future research should investigate the reproducibility of these findings using alternative atlases. Moreover, our analysis was limited to functional connectivity, and the inclusion of structural data could provide a more comprehensive understanding of DMN heterogeneity. The current methodology for assessing IVFC had limited descriptive power, underscoring the necessity for the development of advanced techniques to measure individual variability with greater precision. Additionally, despite the use of the Combat algorithm for site harmonization, residual site effects were observed, indicating the necessity for further optimization of cross-site harmonization strategies. Finally, a key limitation of this study is that it does not account for potential subtypes of IVFC patterns of the DMN regions. Future research should focus on identifying distinct IVFC subtypes across DMN regions and exploring their associations with symptom dimensions in MDD, which may provide a more nuanced understanding of the disorder's heterogeneity.

Conclusion

The present study revealed abnormalities in the DMN of MDD patients by examining increased IVFC, which may reflect greater dysfunction in DMN connectivity. Through transcriptional neuroimaging correlation analyses, we identified biological processes potentially driving these IVFC alterations. These findings highlighted

the variability of the default mode network (DMN) in MDD and provided insight into understanding the neural mechanisms underlying MDD.

Data availability

The data used during the present study could be obtained from open dataset (http://rfmri.org/REST-meta-MDD). The transcriptomic data were obtained from the Allen Human Brain Atlas (https://human.brain-map.org/).The dataset includes six human adult donors (accession numbers: H0351.2001, H0351.2002, H0351.1009, H0351.1012, H0351.1015, H0351.1016).

Received: 18 October 2024; Accepted: 3 March 2025
Published online: 14 March 2025

References

1. Buch, A. M. & Liston, C. Dissecting diagnostic heterogeneity in depression by integrating neuroimaging and genetics. *Neuropsychopharmacology* **46**, 156–175. https://doi.org/10.1038/s41386-020-00789-3 (2021).
2. Marx, W. et al. Major depressive disorder. *Nat. Rev. Dis. Primers*. **9**, 44. https://doi.org/10.1038/s41572-023-00454-1 (2023).
3. Jing, R. et al. Heterogeneous brain dynamic functional connectivity patterns in first-episode drug-naive patients with major depressive disorder. *Hum. Brain Mapp.* **44**, 3112–3122. https://doi.org/10.1002/hbm.26266 (2023).
4. Buckner, R. L., Andrews-Hanna, J. R. & Schacter, D. L. The brain's default network: anatomy, function, and relevance to disease. *Ann. N Y Acad. Sci.* **1124**, 1–38. https://doi.org/10.1196/annals.1440.011 (2008).
5. Lee, T. W. & Xue, S. W. Functional connectivity maps based on hippocampal and thalamic dynamics May account for the default-mode network. *Eur. J. Neurosci.* **47**, 388–398. https://doi.org/10.1111/ejn.13828 (2018).
6. Smallwood, J. et al. The default mode network in cognition: a topographical perspective. *Nat. Rev. Neurosci.* **22**, 503–513. https://doi.org/10.1038/s41583-021-00474-4 (2021).
7. Kucyi, A., Kam, J. W. Y., Andrews-Hanna, J. R., Christoff, K. & Whitfield-Gabrieli, S. Recent advances in the neuroscience of spontaneous and off-task thought: implications for mental health. *Nat. Ment. Health*. **1**, 827–840. https://doi.org/10.1038/s44220-023-00133-w (2023).
8. Whitfield-Gabrieli, S. & Ford, J. M. Default mode network activity and connectivity in psychopathology. *Annu. Rev. Clin. Psychol.* **8**, 49–76. https://doi.org/10.1146/annurev-clinpsy-032511-143049 (2012).
9. Kaiser, R. H., Andrews-Hanna, J. R., Wager, T. D. & Pizzagalli, D. A. Large-Scale network dysfunction in major depressive disorder: A Meta-analysis of Resting-State functional connectivity. *JAMA Psychiatry*. **72**, 603–611. https://doi.org/10.1001/jamapsychiatry.2015.0071 (2015).
10. Saris, I. M. J. et al. Default mode network connectivity and social dysfunction in major depressive disorder. *Sci. Rep.* **10**, 194. https://doi.org/10.1038/s41598-019-57033-2 (2020).
11. Scalabrini, A. et al. All roads lead to the default-mode network-global source of DMN abnormalities in major depressive disorder. *Neuropsychopharmacology* **45**, 2058–2069. https://doi.org/10.1038/s41386-020-0785-x (2020).
12. Runia, N. et al. The neurobiology of treatment-resistant depression: A systematic review of neuroimaging studies. *Neurosci. Biobehav. Rev.* **132**, 433–448. https://doi.org/10.1016/j.neubiorev.2021.12.008 (2022).
13. Mueller, S. et al. Individual variability in functional connectivity architecture of the human brain. *Neuron* **77**, 586–595. https://doi.org/10.1016/j.neuron.2012.12.028 (2013).
14. Liao, X., Cao, M., Xia, M. & He, Y. Individual differences and time-varying features of modular brain architecture. *Neuroimage* **152**, 94–107. https://doi.org/10.1016/j.neuroimage.2017.02.066 (2017).
15. Xu, Y. et al. Development and emergence of individual variability in the functional connectivity architecture of the preterm human brain. *Cereb. Cortex*. **29**, 4208–4222. https://doi.org/10.1093/cercor/bhy302 (2019).
16. Li, L. et al. Gene expression associated with individual variability in intrinsic functional connectivity. *Neuroimage* **245** https://doi.org/10.1016/j.neuroimage.2021.118743 (2021).
17. Hou, Z. et al. Linking individual variability in functional brain connectivity to polygenic risk in major depressive disorder. *J. Affect. Disord*. **329**, 55–63. https://doi.org/10.1016/j.jad.2023.02.104 (2023).
18. Elman, J. A. et al. Genetic and environmental influences on cortical mean diffusivity. *Neuroimage* **146**, 90–99 (2017).
19. Yan, C. G. et al. Reduced default mode network functional connectivity in patients with recurrent major depressive disorder. *Proc. Natl. Acad. Sci. U. S. A.* **116**, 9078–9083. https://doi.org/10.1073/pnas.1900390116 (2019).
20. Chen, X. et al. The DIRECT consortium and the REST-meta-MDD project: towards neuroimaging biomarkers of major depressive disorder. *Psychoradiology* **2**, 32–42. https://doi.org/10.1093/psyrad/kkac005 (2022).
21. Hamilton, M. A rating scale for depression. *J. Neurol. Neurosurg. Psychiatry*. **23**, 56–62. https://doi.org/10.1136/jnnp.23.1.56 (1960).
22. Xiao, Y., Zhao, L., Zang, X. & Xue, S. W. Compressed primary-to-transmodal gradient is accompanied with subcortical alterations and linked to neurotransmitters and cellular signatures in major depressive disorder. *Hum. Brain Mapp.* **44**, 5919–5935. https://doi.org/10.1002/hbm.26485 (2023).
23. Dosenbach, N. U. et al. Prediction of individual brain maturity using fMRI. *Science* **329**, 1358–1361. https://doi.org/10.1126/science.1194144 (2010).
24. Hawrylycz, M. J. et al. An anatomically comprehensive atlas of the adult human brain transcriptome. *Nature* **489**, 391–399. https://doi.org/10.1038/nature11405 (2012).
25. Arnatkevičiūtė, A., Fulcher, B. D. & Fornito, A. A practical guide to linking brain-wide gene expression and neuroimaging data. *Neuroimage* **189**, 353–367. https://doi.org/10.1016/j.neuroimage.2019.01.011 (2019).
26. Fortin, J. P. et al. Harmonization of cortical thickness measurements across scanners and sites. *Neuroimage* **167**, 104–120. https://doi.org/10.1016/j.neuroimage.2017.11.024 (2018).
27. Li, J. et al. Cortical structural differences in major depressive disorder correlate with cell type-specific transcriptional signatures. *Nat. Commun.* **12** https://doi.org/10.1038/s41467-021-21943-5 (2021).
28. Sun, X. et al. Disrupted intersubject variability architecture in functional connectomes in schizophrenia. *Schizophr. Bull.* **47**, 837–848. https://doi.org/10.1093/schbul/sbaa155 (2021).
29. Xia, M. et al. Shared and distinct functional architectures of brain networks across psychiatric disorders. *Schizophr. Bull.* **45**, 450–463. https://doi.org/10.1093/schbul/sby046 (2019).
30. Ma, Q. et al. Transdiagnostic dysfunctions in brain modules across patients with schizophrenia, bipolar disorder, and major depressive disorder: A Connectome-Based study. *Schizophr. Bull.* **46**, 699–712. https://doi.org/10.1093/schbul/sbz111 (2020).
31. Hiser, J. & Koenigs, M. The multifaceted role of the ventromedial prefrontal cortex in emotion, decision making, social cognition, and psychopathology. *Biol. Psychiatry*. **83**, 638–647. https://doi.org/10.1016/j.biopsych.2017.10.030 (2018).
32. Zald, D. H., Mattson, D. L. & Pardo, J. V. J. P. O. T. N. A. O. S. Brain activity in ventromedial prefrontal cortex correlates with individual differences in negative affect. **99**, 2450–2454 (2002).

33. Chang, L. J. et al. Endogenous variation in ventromedial prefrontal cortex state dynamics during naturalistic viewing reflects affective experience. **7**, eabf7129. https://doi.org/10.1126/sciadv.abf7129 (2021).
34. Lee, K., Kim, N., Jeong, E. J., Kang, M. S. & Kim, M. J. Volumetric variability of the ventromedial prefrontal cortex reflects the propensity for engaging in High-Stakes gambling behavior. *Brain Sci.* **12** https://doi.org/10.3390/brainsci12111460 (2022).
35. Borsini, A., Wallis, A. S. J., Zunszain, P., Pariante, C. M. & Kempton, M. J. Characterizing anhedonia: A systematic review of neuroimaging across the subtypes of reward processing deficits in depression. *Cogn. Affect. Behav. Neurosci.* **20**, 816–841. https://doi.org/10.3758/s13415-020-00804-6 (2020).
36. Pizzagalli, D. A. & Roberts, A. C. Prefrontal cortex and depression. *Neuropsychopharmacology* **47**, 225–246. https://doi.org/10.1038/s41386-021-01101-7 (2022).
37. Young, C. B. et al. Anhedonia and general distress show dissociable ventromedial prefrontal cortex connectivity in major depressive disorder. *Transl. Psychiatry*. **6**, e810. https://doi.org/10.1038/tp.2016.80 (2016).
38. Ho, T. C. et al. Inflexible functional connectivity of the dorsal anterior cingulate cortex in adolescent major depressive disorder. *Neuropsychopharmacology* **42**, 2434–2445. https://doi.org/10.1038/npp.2017.103 (2017).
39. Journee, S. H., Mathis, V. P., Fillinger, C., Veinante, P. & Yalcin, I. Janus effect of the anterior cingulate cortex: pain and emotion. *Neurosci. Biobehav. Rev.* **153**, 105362. https://doi.org/10.1016/j.neubiorev.2023.105362 (2023).
40. Philippi, C. L., Motzkin, J. C., Pujara, M. S. & Koenigs, M. Subclinical depression severity is associated with distinct patterns of functional connectivity for subregions of anterior cingulate cortex. *J. Psychiatr. Res.* **71**, 103–111. https://doi.org/10.1016/j.jpsychires.2015.10.005 (2015).
41. Zhang, Y. et al. Functional impairment-based segmentation of anterior cingulate cortex in depression and its relationship with treatment effects. *Hum. Brain Mapp.* **42**, 4035–4047. https://doi.org/10.1002/hbm.25537 (2021).
42. Rolls, E. T. et al. Functional connectivity of the anterior cingulate cortex in depression and in health. *Cereb. Cortex*. **29**, 3617–3630. https://doi.org/10.1093/cercor/bhy236 (2019).
43. Zheng, H. et al. The dynamic characteristics of the anterior cingulate cortex in resting-state fMRI of patients with depression. *J. Affect. Disord*. **227**, 391–397. https://doi.org/10.1016/j.jad.2017.11.026 (2018).
44. Weiner, K. S. & Grill-Spector, K. Sparsely-distributed organization of face and limb activations in human ventral Temporal cortex. *Neuroimage* **52**, 1559–1573. https://doi.org/10.1016/j.neuroimage.2010.04.262 (2010).
45. Morris, J. P., Pelphrey, K. A. & McCarthy, G. Face processing without awareness in the right fusiform gyrus. *Neuropsychologia* **45**, 3087–3091. https://doi.org/10.1016/j.neuropsychologia.2007.05.020 (2007).
46. Surguladze, S. et al. A differential pattern of neural response toward sad versus happy facial expressions in major depressive disorder. *Biol. Psychiatry*. **57**, 201–209. https://doi.org/10.1016/j.biopsych.2004.10.028 (2005).
47. Chen, C. et al. Decreased cortical folding of the fusiform gyrus and its hypoconnectivity with sensorimotor areas in major depressive disorder. *J. Affect. Disord*. **295**, 657–664. https://doi.org/10.1016/j.jad.2021.08.148 (2021).
48. Leech, R. & Sharp, D. J. The role of the posterior cingulate cortex in cognition and disease. *Brain* **137**, 12–32. https://doi.org/10.1093/brain/awt162 (2014).
49. Yang, R. et al. Decreased functional connectivity to posterior cingulate cortex in major depressive disorder. *Psychiatry Res. Neuroimaging*. **255**, 15–23. https://doi.org/10.1016/j.pscychresns.2016.07.010 (2016).
50. Cheng, W. et al. Increased functional connectivity of the posterior cingulate cortex with the lateral orbitofrontal cortex in depression. *Transl Psychiatry*. **8**, 90. https://doi.org/10.1038/s41398-018-0139-1 (2018).
51. Zhu, Z. et al. Hyperconnectivity between the posterior cingulate and middle frontal and Temporal gyrus in depression: based on functional connectivity meta-analyses. *Brain Imaging Behav.* **16**, 1538–1551. https://doi.org/10.1007/s11682-022-00628-7 (2022).
52. Li, J. et al. Abnormal activation of the occipital lobes during emotion picture processing in major depressive disorder patients. *Neural Regen. Res.* **8**, 1693–1701. https://doi.org/10.3969/j.issn.1673-5374.2013.18.007 (2013).
53. Lee, J. S. et al. Alterations in the occipital cortex of Drug-Naive adults with major depressive disorder: A surface-Based analysis of surface area and cortical thickness. *Psychiatry Investig.* **18**, 1025–1033. https://doi.org/10.30773/pi.2021.0099 (2021).
54. Liu, D. Y. et al. From molecular to behavior: higher order occipital cortex in major depressive disorder. *Cereb. Cortex*. **32**, 2129–2139. https://doi.org/10.1093/cercor/bhab343 (2022).
55. Song, X. M. et al. Reduction of higher-order occipital GABA and impaired visual perception in acute major depressive disorder. *Mol. Psychiatry*. **26**, 6747–6755. https://doi.org/10.1038/s41380-021-01090-5 (2021).
56. Lin, J. et al. Linking inter-subject variability of cerebellar functional connectome to clinical symptoms in major depressive disorder. *J. Psychiatr. Res.* **171**, 9–16. https://doi.org/10.1016/j.jpsychires.2024.01.006 (2024).
57. Ormel, J., Hartman, C. A. & Snieder, H. The genetics of depression: successful genome-wide association studies introduce new challenges. *Transl. Psychiatry*. **9**, 114 (2019).
58. Limon, A., Mamdani, F., Hjelm, B. E., Vawter, M. P. & Sequeira, A. Targets of polyamine dysregulation in major depression and suicide: Activity-dependent feedback, excitability, and neurotransmission. *Neurosci. Biobehav. Rev.* **66**, 80–91. https://doi.org/10.1016/j.neubiorev.2016.04.010 (2016).
59. Müller, C. P. et al. Brain membrane lipids in major depression and anxiety disorders. *Biochim. Biophys. Acta*. **1851**, 1052–1065. https://doi.org/10.1016/j.bbalip.2014.12.014 (2015).
60. Yan, Z. & Rein, B. Mechanisms of synaptic transmission dysregulation in the prefrontal cortex: pathophysiological implications. *Mol. Psychiatry*. **27**, 445–465 (2022).
61. Fries, G. R., Saldana, V. A., Finnstein, J. & Rein, T. Molecular pathways of major depressive disorder converge on the synapse. *Mol. Psychiatry*. **28**, 284–297. https://doi.org/10.1038/s41380-022-01806-1 (2022).

Acknowledgements

This work was supported by the Key Clinical Specialty Construction Project of Zhejiang Province and the Key Medical Disciplines of Hangzhou. The authors thank the DIRECT consortium for collecting and sharing the data.

Author contributions

C.Y. and S.-W.X. conceived and designed the study. C.Y. and Y.X. analyzed the data. C.Y. wrote the manuscript. C.Y., P.W., S.-W.X., Y.Z., J.P., Y.M., J.W. revised the manuscript. All authors have contributed to and have approved the final manuscript.

Declarations

Competing interests

The authors declare no competing interests.

Additional information

Correspondence and requests for materials should be addressed to S.-W.X.

Reprints and permissions information is available at www.nature.com/reprints.

Publisher's note Springer Nature remains neutral with regard to jurisdictional claims in published maps and institutional affiliations.

Open Access This article is licensed under a Creative Commons Attribution-NonCommercial-NoDerivatives 4.0 International License, which permits any non-commercial use, sharing, distribution and reproduction in any medium or format, as long as you give appropriate credit to the original author(s) and the source, provide a link to the Creative Commons licence, and indicate if you modified the licensed material. You do not have permission under this licence to share adapted material derived from this article or parts of it. The images or other third party material in this article are included in the article's Creative Commons licence, unless indicated otherwise in a credit line to the material. If material is not included in the article's Creative Commons licence and your intended use is not permitted by statutory regulation or exceeds the permitted use, you will need to obtain permission directly from the copyright holder. To view a copy of this licence, visit http://creativecommons.org/licenses/by-nc-nd/4.0/.

© The Author(s) 2025